Marine Pollution Bulletin 178 (2022) 113647

Contents lists available at ScienceDirect

Marine Pollution Bulletin

journal homepage: www.elsevier.com/locate/marpolbul

Weathering indices of microplastics along marine and coastal sediments from the harbor of Cartagena (Spain) and its adjoining urban beach

Javier Bayo *, Dolores Rojo, Sonia Olmos

Department of Chemical and Environmental Engineering, Technical University of Cartagena, Paseo Alfonso XIII 44, E-30203 Cartagena, Spain

ARTICLE INFO

Keywords:
Microplastic
Sediment
Carbonyl index
Vinyl index
Crystallinity

ABSTRACT

Marine and coastal sediments from the harbor of Cartagena (Spain) and its adjoining beach were investigated regarding their microplastic burden. Fibers accounted for 47.62% and 61.66% in marine and coastal sediments, respectively, followed by films (31.43% and 18.76%) and fragments (20.95% and 18.65%). Polyvinyl (36.07%), polypropylene (21.31%), and polyethylene (18.03%) were isolated for marine sediments, and low-density polyethylene (40.71%), polypropylene (20.16%), and acrylate (11.37%) for coastal sediments. Highest concentrations were found in the deepest marine sediments (24.0 m) and in the furthest zone from the seashore for coastal sediments (18 m). Carbonyl index increased in the intermediate area (12.5 m) for marine sediments (0.51), whilst vinyl index was maximum for the deepest samples (1.94), reporting Norrish type I and II reactions, respectively. Coastal sediments collected close to the high tide line displayed the highest average values for both indices, 1.57 and 1.29, respectively, indicating a higher exposition to weathering variables.

1. Introduction

Global plastics production has been increased from 348 million tons in 2017 towards 359 million tons in 2018, almost reaching 370 million tons in 2019 (PlasticsEurope, 2020). Human activities, including packaging, building, construction, spillage during handling, transfer and loss during transportation, or an inefficient end-of-life management, among others, are responsible for the presence of million microplastic particles in our oceans (Veerasingam et al., 2016). Although it is not possible to give exact quantities of manufactured plastic material discarded or washed into the sea or coastal areas, the estimations include that only 15% is floating on the surface of the sea, 15% is hovering in the water column, and 70% will sink and accumulate on the sea bottom (Kurtela and Antolović, 2019), especially those with a density that exceeds that of seawater (1020 kg m^{-3}) (Woodall et al., 2015).

Plastics between 1 μm and 5 mm (particulate), or 3 μm and 15 mm (fibers) are named microplastics (ECHA, 2019), and they are divided into two different groups: primary microplastics, purposefully manufactured for commercial use in personal care products, plastic pellets or nurdles for industrial manufacturing or powders for injection molding; and secondary microplastics, formed in the process of weathering and disintegration of larger plastic particles under the influence of the sun, salt water, waves and other abiotic and biotic factors (Moore, 2008; Kershaw et al., 2019). In this sense, coastline has been spotted as a significant reservoir for their accumulation and release to the sea (Bronzo et al., 2021). Eriksen et al. (2014) have estimated a minimum of 5.25 trillion plastic particles weighing 268,940 tons floating in the world oceans, with a tremendous loss of microplastics from the sea surface compared to expected rates of fragmentation, surely due to different mechanisms that remove these tiny particles from the surface.

Microplastics in the marine environment undergo physical, chemical, and biological degradation. Ultraviolet radiation, under 400 nm wavelength, accelerates polymer degradation because of photolytic, photo-oxidative, and thermo-oxidative reactions, and in seashore, plastics such as polyethylene and polypropylene will also be degraded by physical abrasion because of wave action and sand grinding (Wang et al., 2016). Furthermore, all these processes could be coupled with a biotic degradation, with bacteria and fungi producing a variety of enzymes capable of degrading natural and synthetic polymers (Sánchez, 2020).

Different weathering indices have been proposed to measure chemical changes associated with microplastic aging and degradation. Carbonyl and vinyl indices were probably the first indicators used to measure the chemical oxidation of polyolefins such as polyethylene and polypropylene, generally considered to reflect the degradation of the mechanical properties of these polymers (Mellor et al., 1973). It has

* Corresponding author.
E-mail address: javier.bayo@upct.es (J. Bayo).

https://doi.org/10.1016/j.marpolbul.2022.113647
Received 16 November 2021; Received in revised form 14 February 2022; Accepted 3 April 2022
Available online 13 April 2022

been postulated that carbonyl groups are the main light-absorbing species responsible for the photochemical initiation reactions of UV-exposed polyolefins, following Norrish type I and II reactions (Gardette et al., 2013). When ketones degradation undergoes a Norrish type I reaction, the resulting free radicals may lead to the formation of carboxylic acids, esters, or lactones via crosslinking, or may originate chain scission. Conversely, Norrish type II reaction results in the formation of terminal vinyl groups, acetone, as well as chain scissions (Stark and Matuana, 2004). The crystallinity of polyolefins strongly fluctuates due to chemical changes occurred during weathering processes, increasing with carbonyl index. An early stage of degradation involves controlled chain cleavage, which proceeds with the scission of the entangled molecules during the amorphous phase, leading to a rearrangement of the released segments (Rajakumar et al., 2009).

This paper deals with the occurrence and spatial distribution of microplastics along the sediments in the harbor of Cartagena (Spain) and its adjoining urban beach. Collected microplastics from both marine and coastal sediments were characterized in terms of color, shape, and size, and polymer types were identified by Attenuated Total Reflectance-Fourier Transform Infrared Spectroscopy (ATR-FTIR). The three main objectives of this study were: (1) to characterize microplastic distribution at different sampling points from both marine and coastal sediments; (2) to understand the correlation between weathering processes taking place in their surface and their spatial distribution; and (3) to relate crystallinity changes with carbonyl and vinyl indices. The results of this study will provide insights on the contamination of marine and coastal sediments, as well as spatial factors affecting abundance, deterioration, and characteristics of microplastic burden, linking crystallinity changes to weathering indices to provide an increased understanding for these processes.

2. Materials and methods

2.1. Sampling marine and coastal sediments

Marine sediments close to the harbor of Cartagena, a three-millenary city located in a natural bay in the Southeast of Spain, were collected during March, June, and September 2019 at three different sampling points (Fig. 1), named P1 (37°34′47.04″ N, 0°58′34.62″ W), P2 (37°35′36.72″ N, 0°58′49.20″ W), and P3 (37°34′29.58″ N, 0°58′31.50″ W), with 8.0, 12.5, and 24.0 m in depth, respectively. The three sampling sites differ in their main activities, representing different marine environments also related to depth and hydrodynamic energy levels. Sandy bottoms are the predominant sedimentary cover in P1, located in front of Cala Cortina, a urban beach also monitored in this study; P2 is located in the dock of Cartagena, close to the city, and it includes a recreational and fishing port, and a cruise terminal with 700 m mooring line and 11.25 m draft, with muddy bottom sediments; and P3, named Escombreras dock, located 1.5 miles far from the city port, including LNG (Liquefied Natural Gas) and LPG (Liquefied Petroleum Gas) terminals, supertankers docking for crude oil discharge, and terminals for loading vegetable oils and bioethanol, with more than 5000 m mooring line and 21.40 draft (Fig. S1).

Each time, a surface of 0.04 m^2 was sampled by means of a Van Veen hand-operated grab sampler (Fig. S2), the most frequently used tool for benthic sediment collection (Claessens et al., 2011; Razeghi et al., 2021), on board a speedboat guided by a pocket-size Garmin GPS. Samples were subsequently subsampled in triplicate and placed into sterilized glass vessels with metallic lid, until arrival into the laboratory. Marine sediments were dried overnight a 60 °C in a forced air stove FD 23 (Binder GmbH, Tuttlingen, Germany), then sieved on a 5 mm mesh sieve and stored at 4 °C in glass sealed containers before microplastic extraction.

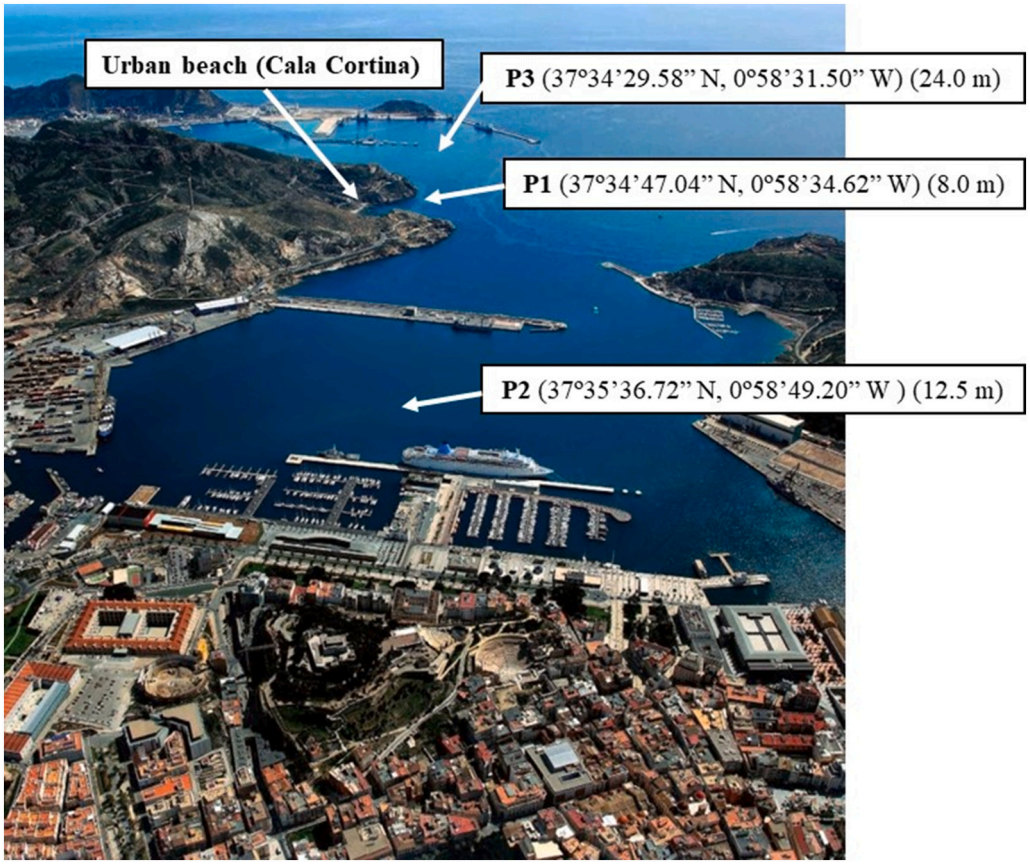

Fig. 1. Location of three sampling points for marine sediments monitored in this study.

Coastal sediments were also collected at three sampling points within the Cala Cortina urban beach (Fig. 2); named Z1, close to the high tide line (37°34′52.94″ N, 0°58′29.88″ W); Z2, 9 m landward from high tide line (37°34′53.17″ N, 0°58′29.67″ W); and Z3, 18 m landward from high tide line (37°34′53.46″ N, 0°58′29.50″ W). Triplicate samples of 0.25 m^2 quadrats were collected placing a square of 0.50 m with the aid of a metal trowel, during March, June, and September 2019. Samples were always collected from the superficial layer included within the sampling frame (maximum depth 3–4 cm) and placed into 120-mm glass Petri dishes, with an average amount (±SE) of 226.8 (±5.7) g (dw), and minimum and maximum values of 193.3 and 265.3 g (dw) (Fig. S3).

2.2. Measurement of microplastics in marine and coastal sediments

All sample processing was conducted avoiding plastic lab devices to the maximum, and all glassware was thoroughly washed with tap water and twice with deionized water after each experiment, covering it with aluminum foil to mitigate contamination. Only natural fiber clothing and cotton coats were worn in the lab for sample processing.

Fifty grams of dry marine sediment was each time analyzed for microplastics. Biofilm removal from their surfaces was carried out by adding 100 ml of 10% KOH solution in 250 ml glass beakers, at 40 °C for 48 h. Dehaut et al. (2016) and Kühn et al. (2017) have reported that most of polymers identified from beaches and marine debris were resistant against KOH, recommending its use for microplastic research. Digested, samples were resuspended in 100 ml of 2.05 M NaCl solution (density: 1080 kg m^{-3}) (Panreac, Barcelona, Spain) and mechanically stirred in a jar-test device (300 rpm, 20 min), for a further extraction based on density floatation. After 20 min of settlement, the supernatant was vacuum filtered through a Büchner funnel using a paper filter (Prat Dumas, Couze-St-Front, France, diameter 110 mm, pore size 0.45 mm). The funnel wall was twice washed with deionized water and also filtered. Isolated microplastic particles were recovered by orbital shaking (150 rpm, 30 min), placing filters into 120-mm glass Petri dishes after washing with 15 ml deionized water. Samples were dried overnight at 60 °C in a forced air stove FD 23 (Binder GmbH, Tuttlingen, Germany), and kept in a desiccator to avoid moisture. Coastal sediments were similarly processed for microplastic extraction, although without the digestion process, as previously reported in Bayo et al. (2019) for sand sediments in the Mar Menor coastal lagoon.

Besides, negative control samples or procedural blank measurements were analyzed throughout the study, by vacuum filtering a mixture of 10% KOH (100 ml), 2.05 M NaCl solution (250 ml), and 150 ml of deionized water through a clean paper filter, to determine any potential microplastic contamination during the lab work. No microplastics were identified from blank samples.

After visual identification under an Olympus SZ-61TR Zoom Trinocular Microscope (Olympus Co., Tokyo, Japan) coupled to a Leica MC190 HD digital camera and an image capturing software Leica Application Suite (LAS) 4.8.0 (Leica Microsystems Ltd., Heerbrugg, Switzerland), all isolated microparticles were analyzed to identify polymer types and their weathering processes by means of a Thermo Nicolet 5700 Fourier transformed infrared (FTIR) spectrometer (Thermo Nicolet Analytical Instruments, Madison, WI, USA), provided with a deuterated triglycine sulfate, DTGS, detector and KBr optics. The spectra collected by attenuated total reflectance (ATR) were an average of 20 scans with a resolution of 16 cm^{-1} in the range of 400–4000 cm^{-1}. Spectra were controlled and evaluated by the OMNIC software without further manipulations, and polymers were identified by means of different reference polymer libraries, containing spectra of all common polymers; i.e., Hummel Polymer and Additives (2011 spectra), Polymer Additives and Plasticizers (1799 spectra), Sprouse Scientific Systems Polymers by ATR Library (500 spectra), and Rubber Compounding Materials (350 spectra). A hit quality percentage match >60% was used as the threshold for polymer identification. Finally, total organic carbon (TOC) was measured by means of a TOC analyzer (Shimadzu TOC-V CSH).

2.3. Weathering indexes

Spectra obtained by ATR-FTIR for polymers with saturated alkyl chains, such as polyethylene (PE), both low-density (LDPE) and high-density polyethylene (HDPE), polypropylene (PP), and polyethylene polypropylene copolymer (PEP) were used to estimate the carbonyl and vinyl indices, representing further degradation of the polymer with higher values of both indices. Carbonyl index is defined as the absorbance of the carbonyl peak at 1722–1712 cm^{-1} relative to that of the asymmetric tensile 2H vibration of methylene group (2910–2900 cm^{-1}). It is used as an indicator of the degree of polymer oxidation (Matsuguma et al., 2017; Miranda et al., 2021), because of the introduction of a carbonyl group into the chemical structure, and the peak between 2910 and 2900 cm^{-1} can serve as a reference because it remains unchanged during degradation (Andrady et al., 1993). Therefore, the carbonyl index was used for the quantification of weathering processes of

Fig. 2. Location of three sampling points for coastal sediments monitored in this study.

indicated polymers, although it could not be used for polyethylene terephthalate (PET) because of a systematic common peak at 1714 cm^{-1} band due to C═O stretching (Miranda et al., 2021). Vinyl index was calculated as the peak intensity for the vinyl group 910–900 cm^{-1} relative to that of methylene group (2910–2900 cm^{-1}) (Stark and Matuana, 2004; Miranda et al., 2021). In all cases, the FTIR analysis was carried out using an integration method which considers the area below the absorbance peak at the considered band maximum by means of a tangential approach, further applying a baseline correction (Hofko et al., 2018).

The crystallinity of polyethylene microplastics was monitored with the method described by Zerbi et al. (1989), where double peaks observed at 1474–1464 cm^{-1} and 730–720 cm^{-1} correspond to the crystalline content; both 1474 and 730 cm^{-1}, and the amorphous content; both 1464 and 720 cm^{-1}. As proposed by other authors (Colomw et al., 2000; Kaci et al., 2001), the bands at 730 and 720 cm^{-1} were the most appropriate ones for the study, because an asymmetric behavior of bands 1474 and 1464 cm^{-1} (Kaci et al., 2001) besides an interference of bands 1474 and 1464 cm^{-1} with peak from cellulose at 1430 cm^{-1} (Colomw et al., 2000). The following formula was used:

$$X = 100 - \frac{\frac{1-I_a/I_b}{1.233}}{1 + I_a/I_b} * 100$$

where I_a and I_b represents the doublet peaks 730 and 720 cm^{-1}, respectively.

2.4. Statistical analysis of experimental data

Statistical treatment of data was carried out with the SPSS (Statistic Package for Social Science) 26.0 statistic software (IBM Co. Ltd., USA). All data were expressed as mean ± standard error (SE). The fitting performance of one-way analysis of the variance (ANOVA) was computed by means of *F-test*, and Fisher's Least Significance Difference (LSD) test was applied when *F-test* reported rejection of null hypothesis (H_0) to compare paired data and identify statistically significant differences. The nonparametric Kruskal Wallis test was used of the data did not meet the assumptions for the one-way ANOVA. Besides, the fitting performance of different proposed models was assessed by *F-test*, correlation coefficient (R), determination coefficient (R^2), standard error of the estimate (S_e), regression sum of squares (SS_{REG}), and residual sum of squares (SS_{RES}). The adjusted determination coefficient (R^2_{adj}) was a useful index for comparing the explanatory power of different models (Bayo et al., 2009). Residual values of the models were evaluated for independence by means of the Durbin-Watson test (Rutledge and Barros, 2002), and predicted versus measured values allowed us to test the accuracy of each model. Critical value for statistical significance was set at $p < 0.05$.

3. Results and discussion

3.1. Distribution of microplastics in marine sediments

Microplastics were observed at all the three sampling points selected (Fig. 3), with a mean (±standard error) concentration of 19.37 (±2.43) items kg^{-1} dw (dry weight), increasing with depth, i.e., 16.57 (±2.96), 17.45 (±5.06), and 23.78 (±4.59) items kg^{-1} dw (dry weight) for P1, P2, and P3, respectively. Besides, the deeper the sampling point, the larger the dominant size of microplastics was, i.e., 1.02 (±0.11), 1.22 (±0.19), and 1.40 (±0.29) mm for P1, P2, and P3, respectively. In shallow sediments, an easier resuspension of small-sized microplastics

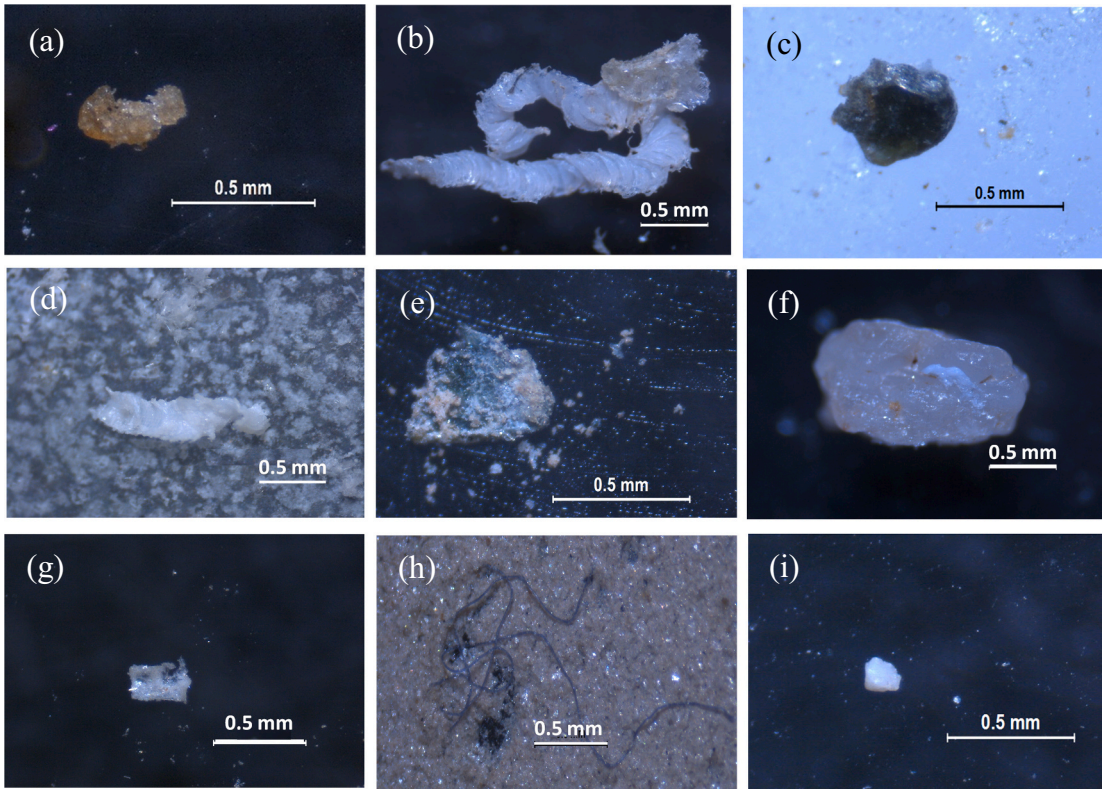

Fig. 3. Microplastics isolated in marine (a–e) and coastal (f–i) sediments identified by FT IR: (a) Ethylene-vinyl acetate (P3/June) (Polymer Additives and Plasticizers); (b) Polypropylene, isotactic (P3/June) (Hummel Polymer and Additives); (c) Acrylamide (P1/March) (Sprouse Polymers by ATR); (d) Low-density polyethylene (P1/September) (Synthetic Fibers by Microscope); (e) Teflon (P2/March) (HR Polymer Additives and Plasticizers); (f) Low-density polyethylene (Z1/March) (Sprouse Polymers by ATR); (g) Acrylate (Z1/June) (HR Polymer Additives and Plasticizers); (h) Poly(ethylene terephthalate) (Z3/June) (Sprouse Polymers by ATR); (i) Polypropylene amorphous (Z2/September) (Polymer Additives and Plasticizers).

may promote their transportation to the water column (Quinn et al., 2017), with a lower concentration than that recorded in deeper sediments, as reported by Adams et al. (2021) in marine sediments of the Canadian Artic. Migration favored by fish ingesting microplastics near the surface and egesting faecal aggregates at depth (Lusher et al., 2016), or fouling mechanisms, especially for microplastics with large surface area to volume ratios (Fazey and Ryan, 2016), may determine the microplastics fate with profundity.

The average of MP sampled in three sampling areas was in the range of $66{\cdot}10^6$ to $95{\cdot}10^6$ items km^{-2}, in good agreement with data reported for the North Atlantic Subtropical Gyre (10^6 MP km^{-2}) (Eriksen et al., 2014) or by Vega-Moreno et al. (2021) in the water column of Canary Islands ($50{\cdot}10^6$ MP km^{-2}). The higher abundance and size of microplastics with depth has also been previously reported (Isobe et al., 2017; Matsuguma et al., 2017; Woodall et al., 2015), suggesting sediments to be the missing link for microplastics in the sea. Nonetheless, the estimated concentration in marine sediments from around the world may vary significantly because of different factors, including the lack of standardized sampling protocol that makes difficult the comparability of data.

The mostly distributed shape of microplastics in marine sediments was fiber (47.62%; 9.57 ± 2.07 items kg^{-1} dw), followed by film (31.43%; 6.05 ± 0.95 items kg^{-1} dw), and fragment (20.95%; 3.75 ± 0.79 items kg^{-1} dw) (Fig. 4a). The smallest size corresponded to a transparent film from P1 (210 μm), and the largest one to a fiber from P3 (9.00 mm). The average proportion of white microplastics was 44.76% across samples, followed by blue shapes (30.48%), although brown (7.62%), red (4.76%), green (4.76%), and black (3.81%) ones were also detected (Fig. 4b).

Twelve different polymer families were identified (Fig. 4c) and, like other studies in harbor sediments (Claessens et al., 2011), polyvinyl (PV) (3.69 ± 1.09 items kg^{-1} dw; 36.07%), polypropylene (PP) (2.52 ± 0.76 items kg^{-1} dw; 21.31%), and polyethylene (PE) (1.90 ± 0.86 items kg^{-1} dw; 18.03%) were the predominant types of microplastic polymers. Lighter polymeric types (PE and PP) were mostly recovered in the shallow sediments, whilst PET in fragmented form was only recovered at the deepest sampling point (P3). PV microplastics were mainly recovered from P1 samples (49.74%) (Fig. 4c). They are ester resins increasingly used as matrix materials for commercial vessels and leisure boats, because of its relative low cost, superior mechanical properties, corrosion resistance and suitability for vacuum molding processing (Thostenson et al., 2009). Most microplastics discharged into the sea eventually sink into the sediments, and their spatial distribution could be related to the polymer density (Harris, 2020; Wang et al., 2019; Zheng et al., 2020), although, as reported by Vega-Moreno et al. (2021), the oceanic dynamics and mesoscale convective flows may overcome the microplastic motion induced by their own buoyancy. In our study, microplastic depth distribution could be also a consequence of some other variables, i.e., a vertical transfer because of anticyclone ridge weather situations prevailing in our region (Cirera et al., 2012), where eddies, especially at their cores where the geostrophic speed is maximum, may transport microplastics (Brach et al., 2018).

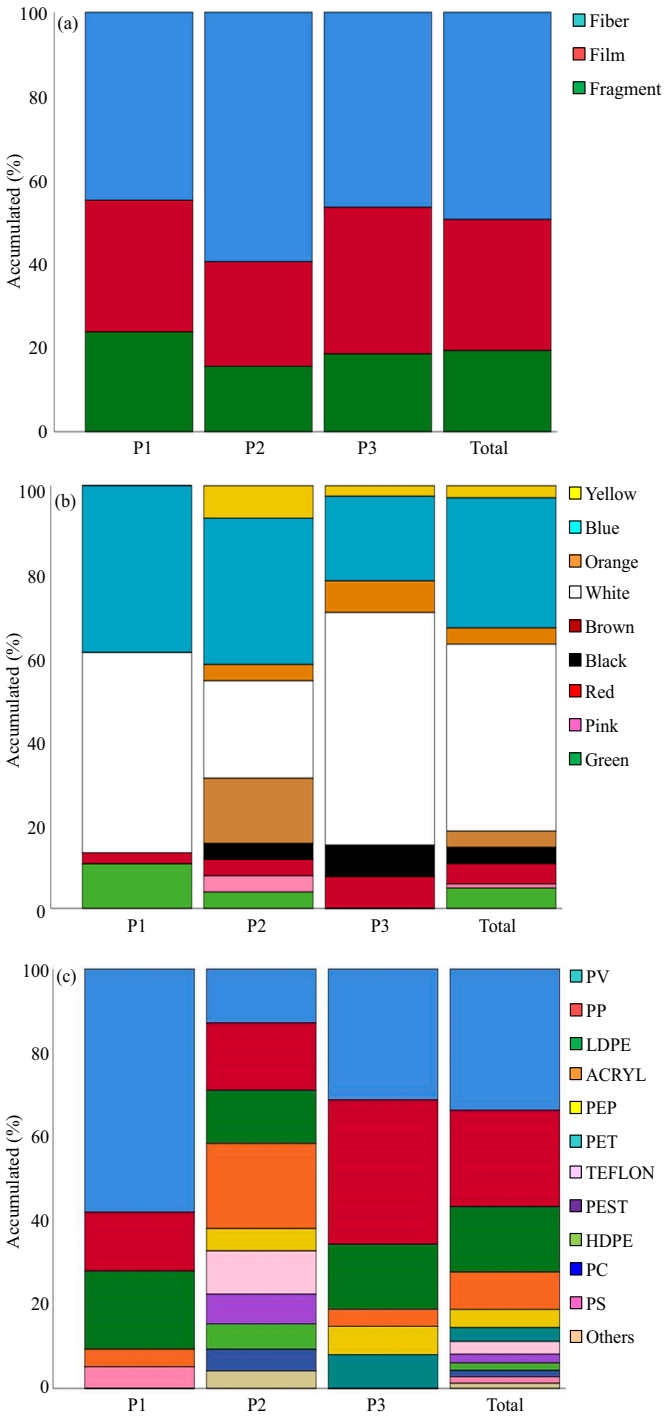

Fig. 4. Accumulated percentages for main characteristics of microplastics isolated in marine sediments: (a) shape categories; (b) colors; (b) polymer types.

3.2. Distribution of microplastics in coastal sediments

The coastal sediment samples from Cala Cortina were characterized by a low organic matter content (TOC = 0.21 ± 0.04%), similar that reported in river sediments from Albania (TOC = 1.4%), beach sediment samples from Scotland (TOC = 0.24%), or India (TOC = 0.06%) (Konechnaya et al., 2021). Identification by FTIR spectroscopy confirmed that average concentration of microplastics was higher for coastal sediments (30.01 ± 7.26 items kg^{-1} dw) than for marine sediments (19.37 ± 2.43 items kg^{-1} dw) previously reported, with minimum and maximum concentrations ranging from 7.98 to 143.23 items kg^{-1} dw. Higher average concentration was reported for Z3 (46.52 ± 20.45 items kg^{-1} dw) than for Z2 (24.74 ± 4.84 items kg^{-1} dw) and Z1 (18.78 ± 3.30 items kg^{-1} dw). Z3 is the furthest point from the shoreline (18 m), close to a car road and a crossing area with high volume of pedestrian traffic and beachgoers, which may contribute to microplastics burden into the ocean. Fig. 5 shows the evolution in the average concentration of microplastics from Z3 to P3, the deepest sampling point for marine sediments. The average microplastics concentration decreased from Z3 to Z1, indicating a clear microplastic distribution with their abundance being highest in the uppermost part of the urban beach (Z3) and decreasing to Z1, the area close to the high tide line, and then revealing a vertical gradient with depth in marine sediments, from P1 to P3. Fiber was the most isolated microplastic shape in coastal

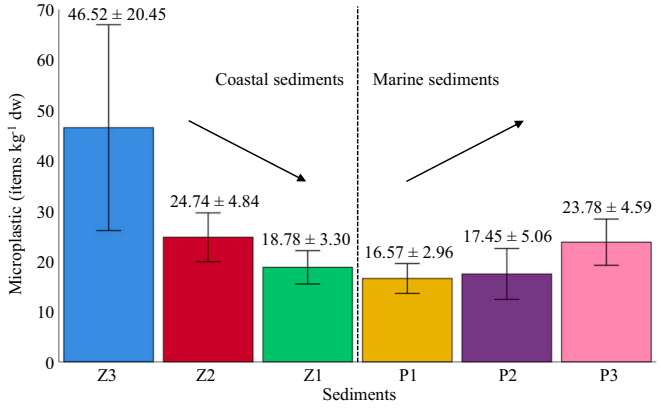

Fig. 5. Average microplastic distribution in marine and coastal sediments (error bars refer to standard error of the mean).

sediments (Fig. 6a) (18.51 ± 4.14 items kg^{-1} dw), accounting for a 61.66% of total types of microplastics, a similar value to that proposed by Sundar et al. (2021) in beach sediments of southernmost India (67%) but lower than that reported by Akkajit et al. (2021) in Phuket, a popular tourism destination in Thailand (85.6%). In our study, Z3 displayed a higher average concentration of fibers (24.94 ± 10.94 items kg^{-1} dw) than Z2 and Z1 (15.29 ± 3.12 items kg^{-1} dw). Film and fragment forms accounted for a 18.76% and 18.65%, respectively, with average concentrations of 5.63 ± 3.22 items kg^{-1} dw and 5.60 ± 1.05 items kg^{-1} dw, respectively. Fragments were statistically more abundant in Z3 (9.43 ± 1.59 items kg^{-1} dw) than in Z2 (5.19 ± 1.56 items kg^{-1} dw) and Z1 (2.17 ± 0.97 items kg^{-1} dw) (*F-test* = 6.758; $p = 0.008$). This fact might be linked to a fragmentation process of large plastic debris (Wagner et al., 2014), and related to proximity to the area with the greatest anthropogenic impact previously discussed, which implies that the presence of microplastics in the coastal sediments is mainly due to human influence, including litter disposal. Only one plastic bead was found in a sample collected in Z1.

A total of 9 polymer families were identified across coastal sediment samples (Fig. 6c). The highest average concentration was by far for LDPE (5.60 ± 1.97 items kg^{-1} dw; 40.71%), followed by PP (2.78 ± 0.86 items kg^{-1} dw; 20.16%), acrylate (ACRYL) (1.56 ± 0.91 items kg^{-1} dw; 11.37%), and HDPE (1.27 ± 0.86 items kg^{-1} dw; 9.26%). Other polymer types; i.e., polyester (PEST), PET, PP, polystyrene (PS), or PV were represented under 1 items kg^{-1} dw. White, blue, red, and black colors accounted for 33.59%, 28.91%, 10.94%, and 7.81% of all analyzed microplastics in coastal sediments, respectively (Fig. 6b). The predominant colors for fiber forms were blue (45.57%), red (17.72%), and white (12.66%), being transparent most of them (86.08%), as previously reported in sand sediment studies in this area (Bayo et al., 2019). Wessel et al. (2016) found 5 polymer types in intertidal sandy samples in Mobile Bay (Alabama, USA), and Yu et al. (2016) and Graca et al. (2017) reported a maximum of 8 types of microplastics in sand samples collected in the Bohai Sea (China) and Southern Baltic Sea, respectively.

3.3. Carbonyl and vinyl indices

Carbonyl and vinyl indices were used to characterize the degree of weathering and surface oxidation of polymers. Results are depicted in Table 1, including minimum, maximum, and average number of each index (±SE). As indicated in Materials and Methods, polyethylene terephthalate (PET) could not be used for carbonyl index calculation because of a systematic common peak at 1714 cm^{-1} band due to C═O stretching (Miranda et al., 2021), that reported abnormally high carbonyl index values, with a minimum of 2.01 and a maximum of 4.71 in both types of sediment. Carbonyl index proved to increase in marine sediments from P1 (0.43 ± 0.07) to P2 (0.51 ± 0.09), and then

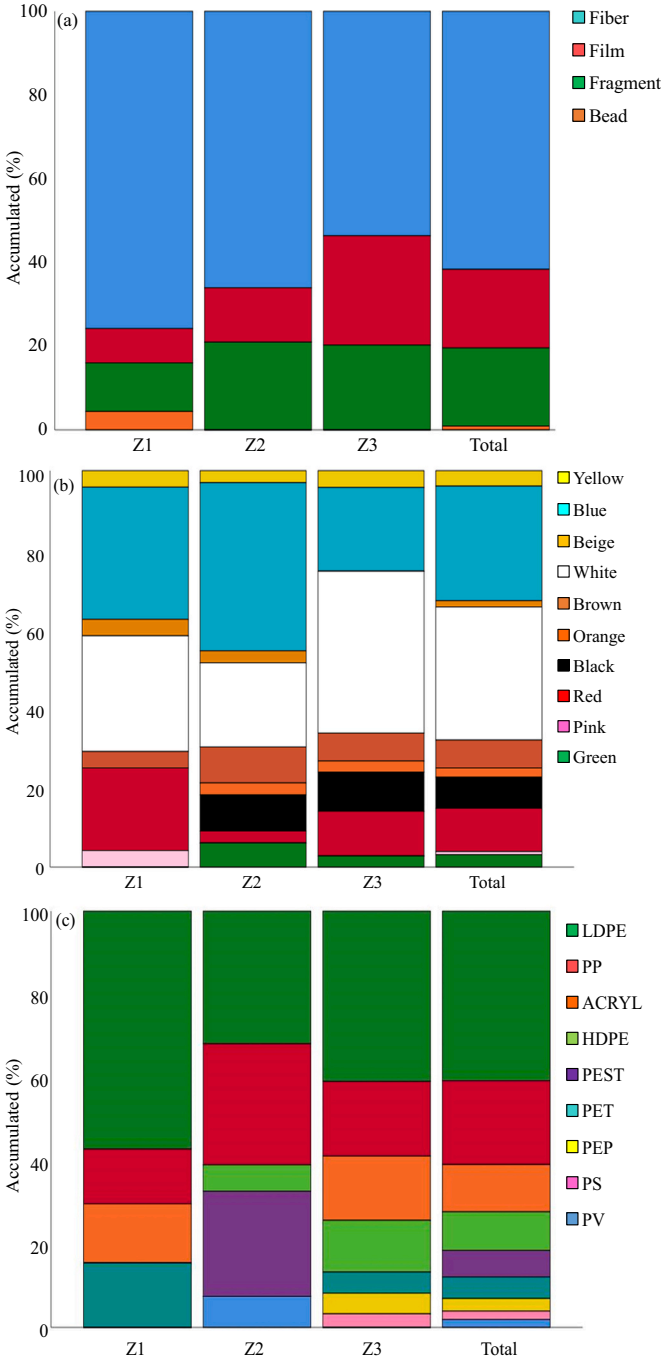

Fig. 6. Accumulated percentages for main characteristics of microplastics isolated in coastal sediments: (a) shape categories; (b) colors; (b) polymer types.

statistically significant decreased to P3 (0.21 ± 0.04) (*F-test* = 5.612; $p = 0.008$). These differences could indicate a protective effect of depth in preventing plastic weathering, with low temperature and a deficiency of solar UV radiation exposure and heat irradiation, both stimulating the sunlight-initiated degradation of microplastics in a natural weathering process (Wang et al., 2016). For PE, no significant differences were reported by sampling site (*F-test* = 3.063; $p = 0.097$), and for PP, site P2 (0.71 ± 0.07) again showed the highest statistically significant average value for carbonyl index (*F-test* = 16.974; $p = 0.001$) with statistically significant differences in pairwise comparisons by LSD test between P2 and P1 (0.37 ± 0.10) ($p = 0.006$), and P2 and P3 (0.23 ± 0.04) ($p = 0.000$). It seems that the initial photodegradation at the shallowest sampling point (P1) evolves towards P2 through a Norrish type I

Table 1
Carbonyl and vinyl indices, and crystallinity for microplastic samples found in marine and coastal sediments.

Sampling location	Site code	Coordinates	Carbonyl index Minimum Maximum Average ± S.E.	Vinyl index Minimum Maximum Average ± S.E.	Crystallinity Minimum Maximum Average ± S.E.
Marine sediments	P1	37°34′47.04″ 0°58′34.62″	0.07 0.81 0.43 ± 0.07	0.74 1.03 0.84 ± 0.07	24.93 70.84 41.65 ± 7.91
	P2	37°35′36.72″ 0°58′49.20″	0.12 0.83 0.51 ± 0.09	0.69 1.80 1.26 ± 0.19	46.30 77.14 63.54 ± 6.74
	P3	37°34′29.58″ 0°58′31.50″	0.08 0.49 0.21 ± 0.04 *F-test* = 5.612 $p = 0.008$	1.57 2.54 1.94 ± 0.08 *F-test* = 19.823 $p = 0.000$	25.52 38.22 33.22 ± 2.97 *F-test* = 5.197 $p = 0.028$
Coastal sediments	Z1	37°34′52.94″ 0°58′29.88″	0.11 1.91 1.57 ± 0.45	0.93 1.78 1.29 ± 0.18	33.98 35.74 34.86 ± 0.88
	Z2	37°34′53.17″ 0°58′29.67″	0.08 1.35 0.35 ± 0.06	0.35 2.20 1.16 ± 0.11	43.93 83.72 63.02 ± 7.39
	Z3	37°34′53.46″ 0°58′29.50″	0.10 0.68 0.28 ± 0.04 *F-test* = 4.025 $p = 0.011$	0.33 1.64 0.77 ± 0.12 *F-test* = 3.724 $p = 0.033$	17.79 86.88 54.44 ± 4.10 *F-test* = 1.743 $p = 0.196$

reaction because of the formation of the carbonyl group, followed by a slower development in the deepest site (P3). Besides, TOC analysis showed a higher average percentage for P2 (0.93 ± 0.07%) than for P1 (0.44 ± 0.04%) or P3 (0.67 ± 0.26%), reflecting the decomposition of polymer chains into the marine sediment (Maes et al., 2017).

There also appears to be a statistically significant difference between sampling months in marine sediments according to carbonyl index. Samples collected in September (0.19 ± 0.02) displayed a lower carbonyl index than those collected in June (0.51 ± 0.06) ($p = 0.000$) and March (0.44 ± 0.09) ($p = 0.008$) (*F-test* = 9.683; $p = 0.001$). It is difficult for external physicochemical factors to contribute to the degradation of microplastics in colder than in milder temperatures (Niu et al., 2021).

Degradation of plastic particles is more apt to occur on land than in the oceans, where exposure to UV radiation and mechanical erosion is minimal (Gregory and Andrady, 2003). Carbonyl index in coastal sediments proved to be significantly higher in Z1, the site close to the high-tide line (1.57 ± 0.45), than that in Z2 (0.35 ± 0.06) and Z3 (0.28 ± 0.04) (*F-test* = 4.025; $p = 0.026$). Although three sampling areas are similarly affected by solar radiation and microorganisms, microplastics collected in Z1 are also wave-exposed, with the presence of oxygen in both air and water, involving an increased sensitivity to weathering reactions that results in the formation of carbonyl radicals primarily from the Norrish type I reaction. The creation of carboxylic, ester and ketone groups on Z1 microplastics could be due to solar radiation, photo-degradation, thermal oxidation, and biodegradation (Singh and Sharma, 2008). In addition, Z1 demonstrated a wider range of carbonyl index values than Z2 or Z3, showing that both fresh and degraded microplastics coexist at that sampling point. The lowest maximum value for carbonyl index was for Z3 (0.68), suggesting proximity to increased anthropogenic activity, as previously reported.

Conversely to marine sediments, coastal samples collected in September (0.42 ± 0.09) displayed a statistically significant higher carbonyl index than those collected in any other month (0.26 ± 0.04) (*F-test* = 3.613; $p = 0.025$). September is the typical rainy month in our area (Ruiz-Álvarez et al., 2017), especially during 2019 when strong torments and flood episodes took place (Hermoso et al., 2021) that could carry more degraded microplastics to the beach and enhance their mechanical abrasion. Moreover, rainfall episodes in September may induce a dynamic environment and cause microplastic fragmentation, with a statistically significant smaller average size (0.53 ± 0.08 mm) than in any other month (*F-test* = 7.678; $p = 0.002$). In this sense, a high carbonyl index contributed to the accumulation of the lowest average size. Similar results were reported in sewage systems from our region during rainy episodes (Bayo et al., 2020).

Statistically significant differences in carbonyl index among forms were found for marine sediments (*F-test* = 4.736; $p = 0.016$), namely between films (0.30 ± 0.04) and fragments (0.53 ± 0.09) ($p = 0.014$), and films and fibers (0.57 ± 0.16) ($p = 0.049$). For coastal sediments, differences in carbonyl index among colors and shapes were found for PP (*F-test* = 7.064; $p = 0.017$), with a lower average value for colored films (0.25 ± 0.02) than for white fragments (0.84 ± 0.18) ($p = 0.006$) or white fibers (0.68 ± 0.05) ($p = 0.040$). Differences in average carbonyl index were identified among colors when running Kruskal Wallis test ($p = 0.016$) (Table S1), likely between white and blue (0.2931 vs. 0.5525, $p = 0.037$) and white and green (0.7191, $p = 0.011$) although they disappeared after significance values were adjusted by Bonferroni correction for multiple tests (0.555 and 0.165, respectively) (Table S2). Prata et al. (2020) reported no differences in average carbonyl index by color in microplastics collected in a sandy beach in Portugal, although carbonyl index turned out to be lower for black PP pellets than for yellow particles. Pigments have proven to prevent or at least be protective from plastic chemical weathering, due to the absorption of the harmful UV light and trapping of radicals that change the physical and optical properties of the polymer and acting as an antioxidant in surface sediments (Campanale et al., 2020).

The vinyl index significantly increased in marine sediments from P1 (0.84 ± 0.07) to P2 (1.26 ± 0.19), and then to P3 (1.94 ± 0.08) (*F-test* = 19.823; $p = 0.000$). After a significant decrease of carbonyl index from P2 to P3 previously reported, the formation of vinyl groups via a Norrish type II reaction proved to be statistically favored by depth. The increase formation of carbonyl groups at P2 could lead to a plateau or stabilization at the deepest sampling site (P3), and the delay of secondary carbonyl group formation at P3 conversely resulted in a significant increase in the formation of vinyl groups, as demonstrated by the statistically significant increase in the vinyl index. Besides, the decrease of vinyl index in P1, the shallowest marine sediment, could be due to an easy metabolization of double bonds by microorganisms (Sen and Raut, 2015).

For coastal sediments, vinyl index decreased from Z1 (1.29 ± 0.18)

to Z2 (1.16 ± 0.11), and then to Z3 (0.77 ± 0.12) (*F-test* = 3.724; p = 0.033). These results, combined with an also significant decrease in the carbonyl index from Z1 to Z3 previously reported, may indicate that the massive formation of both carbonyl and vinyl groups in Z1 stemmed from Norrish types I and II reactions, responsible for the whole photocatalytic degradation process. The evolution of carbonyl and vinyl groups are the main indicators for monitoring the degradation degree of a polymer (Tofa et al., 2019) and, interestingly, both indices increased in the same sampling area, Z1, where microplastic undergoes successive and rapid reactions to generate both carbonyl and vinyl containing species. This fact should be also related to the lowest microplastic concentration (18.78 ± 3.30 items kg^{-1} dw) previously reported for Z1. Moreover, fibers displayed a statistically significant lower vinyl index (0.78 ± 0.14) than films (0.92 ± 0.09) and fragments (1.30 ± 0.16) (*F-test* = 3.394; p = 0.035), the latter with the largest exposure surface for being chemically weathered, and both fibers and fragments proved to display a higher average concentration in Z3, the sampling point with the lowest average carbonyl and vinyl indices. Differences among colors were found for average vinyl index (p = 0.003) (Table S1), i.e., between yellow and brown (0.3390 vs. 1.7018, p = 0.011), yellow and black (1.7783, p = 0.038), blue and brown (0.4330, p = 0.001), blue and black (p = 0.027), green and brown (0.6968, p = 0.010), and white and brown (0.9789, p = 0.005), although only significant differences remained for blue and brown, as indicated by Bonferroni correction (p = 0.014) (Table S3). Hence, the presence of carbonyl and vinyl groups confirms the photo-oxidative degradation of polymers, that could lead to the formation of nano-plastics (Acosta-Coley and Olivero-Verbel, 2015). In general, an increase in both carbonyl and vinyl indices reported low microplastic abundances together with small average sizes, especially for coastal sediments, strongly related to important factors taking place simultaneously, such as solar radiation, photo-degradation, thermal oxidation, and biodegradation. However, the results for marine sediments were not so clear, possibly due to milder and more stable environmental conditions, the absence of solar radiation, as well as mesoscale anticyclonic eddies reported in our region.

3.4. Crystallinity changes

Pristine plastic has lower crystallinity than weathered one, indicating that chain scission has occurred: the shorter the chains, the more mobile they are, with an increased and more readily crystallization and associated embrittlement (Stark and Matuana, 2004; Ter Halle et al., 2017; Liu et al., 2021). Generally, because of structure and functional groups destruction after degradation, the crystallinity of polymer increases (Liu et al., 2019). This is consistent with the observation that P2, the sampling point with the highest average carbonyl index for marine sediments (Table 1), also displayed the highest average crystallinity value, with statistically significant differences (*F-test* = 5.197; p = 0.028). In general, marine plastic debris display a higher crystallinity compared to raw packaging material (Ter Halle et al., 2017), being crystallinity increase an indicator of chains scission by oxidation and a subsequent rearrangement of the smaller molecules, undergoing recrystallization towards a more ordered structure (Stark and Matuana, 2004; Fayolle et al., 2008). Although crystallinity did not significantly change by sampling points for coastal sediments (*F-test* = 1.743; p = 0.196) (Table 1) it did in marine sediments, proving to decrease from P2 (63.54 ± 6.74%) to P1 (41.65 ± 7.91%) (p = 0.040) and P2 to P3 (33.22 ± 2.97%) (p = 0.011), the deepest area, as identified by LSD test. In our study, fibers reported the highest average value for crystalline index (67.93 ± 2.70%), followed by films (55.72 ± 3.98%), fragments (40.50 ± 3.01%), and beads (35.73 ± 3.55%) (*F-test* = 3.006; p = 0.043), for both marine and coastal sediments.

3.4.1. Development of regression models

To relate crystallinity changes with carbonyl and vinyl indices, two generalized linear regression models were developed on experimental data (Table 2), according to the following equations for marine (1) and coastal (2) sediments:

$$\text{Crystallinity} = 26.281 + 293.482\text{*Carbonyl Index} - 161.351\text{*Vinyl Index} \quad (1)$$

$$\text{Crystallinity} = 93.398 + 22.845\text{*Carbonyl Index} - 35.297\text{*Vinyl Index} \quad (2)$$

Eqs. (1) and (2) resulted in R^2 values of 0.770 and 0.649, respectively, indicating a clear linear relationship of carbonyl and vinyl indices with crystallinity changes as independent variable, although a significant proportion of the variance remains unexplained. This may lie in the fact that, although all the weathering parameters considered stand for changes in polymers surface, crystallinity variations may affect deeper structural changes, with a higher degradation gradient in the most superficial layers of the polymeric material. Both equations displayed a negative influence of vinyl index, although its inclusion in the equations was necessary, as the models without this index resulted in a lower R^2_{adj}, i.e., 0.341 and 0.038 for marine and coastal sediments, respectively, as compared to 0.719 and 0.621, respectively, when vinyl index is included.

The Durbin–Watson statistic test was used to detect the absence of autocorrelation in the residuals from the regression models. When the Durbin–Watson value converges to zero, there is a strong correlation between the regression residuals. On the contrary, a Durbin–Watson value converging to 2.0 indicates a weak correlation or random distribution between successive points (Rutledge and Barros, 2002). As depicted in Table 2, the Durbin-Watson statistics for marine and coastal sediment models were found to be 2.563 and 1.627, respectively, demonstrating that the residuals were independent.

To validate both models, a residual analysis was also conducted. Fig. 7 depicts normal P–P (Probability-Probability) plots of standardized residuals for observed versus predicted crystallinity values according to both marine (Fig. 7a) and coastal (Fig. 7b) sediments. Both graphs displayed pair of values close to the line, implying the regression standardized residuals are normally distributed and both equations are reasonable and reliable, with any unusual behavior and in accordance with the hypothesis of normal distribution for the errors of the model.

4. Conclusion

Microplastics in marine sediments from the harbor of Cartagena and coastal sediments from its adjoining beach were found in average concentrations of 19.37 and 30.01 items kg^{-1} dw, respectively, with a maximum average abundance in the deepest sampling point for marine sediments (23.78 items kg^{-1} dw) and the sampling point farthest inland from the high tide line selected for coastal sediments (46.52 items kg^{-1} dw). Fiber was the most isolated microplastic shape both in marine and coastal sediments, followed by film and fragment. Twelve and nine different polymer families were isolated for marine and coastal

Table 2
Main statistical parameters defining regression analyses for crystallinity in marine and coastal sediments.

	Marine sediments	Coastal sediments
R	0.878	0.805
R^2	0.770	0.649
R^2_{adj}	0.719	0.621
S_e	8.483	11.416
SS_{REG}	2169.147	6014.313
SS_{RES}	647.651	3258.274
F-test	15.072	23.073
p-value	0.001	0.000
df	11	27
Durbin-Watson	2.563	1.627

(R) correlation coefficient; (R^2) determination coefficient; (R^2_{adj}) adjusted determination coefficient; (S_e) standard error of the estimate; (SS_{REG}) regression sum of squares; (SS_{RES}) residual sum of squares; (df) degree of freedom.

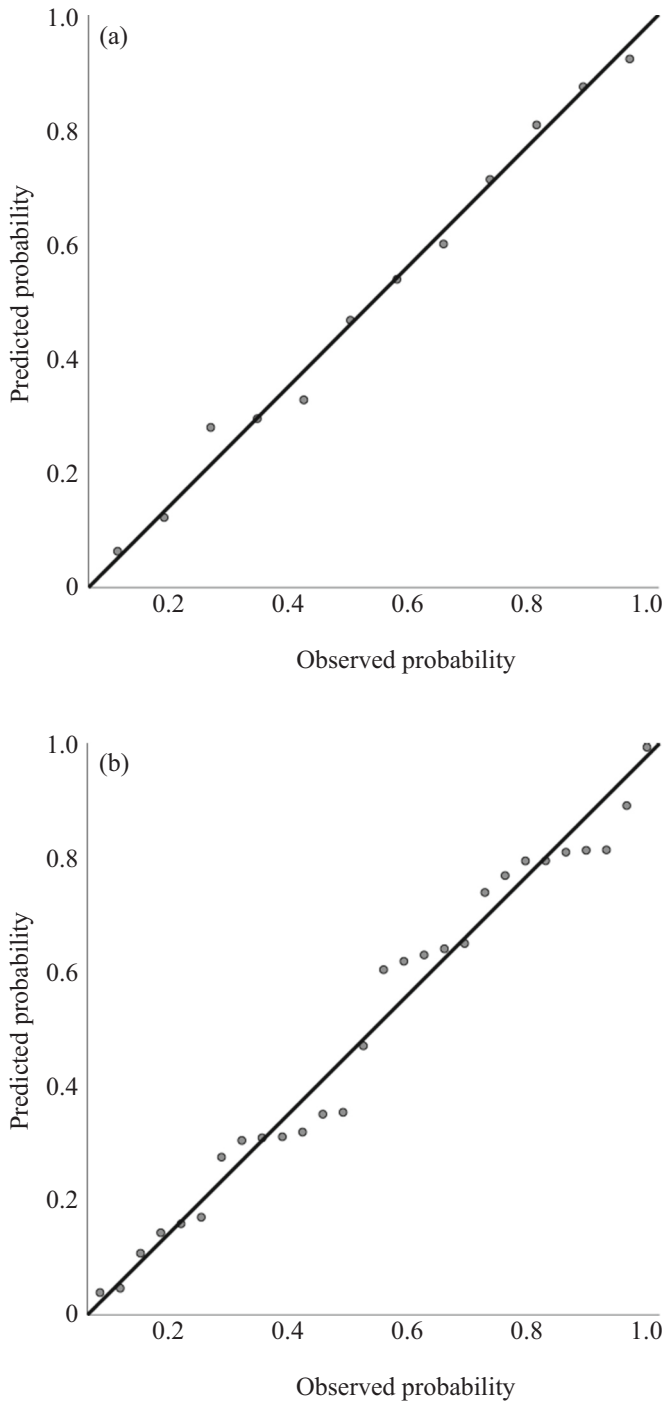

Fig. 7. Relationship between observed versus predicted standardized residues values for (a) marine sediments, and (b) coastal sediments for crystallinity equations.

sediments, respectively, with polyvinyl microplastics for marine sediments and LDPE for coastal sediments being the main ones identified. The carbonyl index was statistically significantly higher in the intermediate zone of marine sediments, although vinyl index proved to increase from shallow to deeper marine sediments. For coastal samples, those collected close to the high tide line displayed the highest carbonyl and vinyl indices, with also the lowest average concentration of microplastics, revealing an important degradation process commanded by different biotic and abiotic factors. The evolution of indices was not as clear in marine sediments, with other mesoscalic factors affecting the whole process. To conclude, both weathering indices could be reliably used to predict changes in crystallinity, although a significant proportion of the variance remained unexplained and should be identified in future studies considering other factors in the experimental design as well.

CRediT authorship contribution statement

Javier Bayo: Methodology, Formal analysis, Writing – original draft, Investigation, Funding acquisition. **Dolores Rojo:** Conceptualization, Methodology, Supervision, Investigation. **Sonia Olmos:** Investigation, Resources, Supervision, Visualization.

Declaration of competing interest

The authors declare that they have no known competing financial interests or personal relationships that could have appeared to influence the work reported in this paper.

Acknowledgements

We thank Pedro Martínez for technical assistance. This work was financially supported by grant 20268/FPI/17 from Fundación Séneca assigned to Dr. Sonia Olmos and by Project Number 5813/19IQA from Cartagena Port Authority.

Appendix A. Supplementary data

Supplementary data to this article can be found online at https://doi.org/10.1016/j.marpolbul.2022.113647.

References

Acosta-Coley, I., Olivero-Verbel, J., 2015. Microplastic resin pellets on an urban tropical beach in Colombia. Environ. Monit. Assess. 187 (7), 1–14.
Adams, J.K., Dean, B.Y., Athey, S.N., Jantunen, L.M., Bernstein, S., Stern, G., Diamond, M.L., Finkelstein, S.A., 2021. Anthropogenic particles (including microfibers and microplastics) in marine sediments of the Canadian Arctic. Sci. Total Environ. 784, 147155.
Akkajit, P., Tipmanee, D., Cherdsukjai, P., Suteerasak, T., Thongnonghin, S., 2021. Occurrence and distribution of microplastics in beach sediments along Phuket coastline. Mar. Pollut. Bull. 169, 112496.
Andrady, A.L., Pegram, J.E., Tropsha, Y., 1993. Changes in carbonyl index and average molecular weight on embrittlement of enhanced-photodegradable polyethylenes. J. Environ. Polym. Degrad. 1 (3), 171–179.
Bayo, J., Angosto, J.M., Gomez-Lopez, M.D., 2009. Ecotoxicological screening of reclaimed disinfected wastewater by Vibrio fischeri bioassay after a chlorination–dechlorination process. J. Hazard. Mater. 172, 166–171.
Bayo, J., Rojo, D., Olmos, S., 2019. Abundance, morphology, and chemical composition of microplastics in sand and sediments from a protected coastal area: the mar menor lagoon (SE Spain). Environ. Pollut. 252, 1357–1366.
Bayo, J., Olmos, S., López-Castellanos, J., 2020. Microplastics in an urban wastewater treatment plant: the influence of physicochemical parameters and environmental factors. Chemosphere 238, 124593.
Brach, L., Deixonne, P., Bernard, M.F., Durand, E., Desjean, M.C., Perez, E., van Seville, E., Ter Halle, A., 2018. Anticyclonic eddies increase accumulation of microplastic in the North Atlantic subtropical gyre. Mar. Pollut. Bull. 126, 191–196.
Bronzo, L., Lusher, A.L., Schøyen, M., Morigi, C., 2021. Accumulation and distribution of microplastics in coastal sediments from the inner Oslofjord, Norway. Mar. Pollut. Bull. 173, 113076.
Campanale, C., Dierkes, G., Massarelli, C., Bagnuolo, G., Uricchio, V.F., 2020. A relevant screening of organic contaminants present on freshwater and pre-production microplastics. Toxics 8 (4), 100.
Cirera, L., García-Marcos, L., Giménez, J., Moreno-Grau, S., Tobías, A., Pérez-Fernández, V., Elvira-Rendueles, B., Guillén, J.J., Navarro, C., 2012. Daily effects of air pollutants and pollen types on asthma and COPD hospital emergency visits in the industrial and Mediterranean spanish city of Cartagena. Allergol. Immunopathol. 40 (4), 231–237.
Claessens, M., De Meester, S., Van Landuyt, L., De Clerck, K., Janssen, C.R., 2011. Occurrence and distribution of microplastics in marine sediments along the Belgian coast. Mar. Pollut. Bull. 62 (10), 2199–2204.
Colomw, X., Cañavate, J., Pagés, P., Saurina, J., Carrasco, F., 2000. Changes in crystallinity of the HDPE matrix in composites with cellulosic fiber using DSC and FTIR. J. Reinf. Plast. Compos. 19 (10), 818–830.
Dehaut, A., Cassone, A.L., Frère, L., Hermabessiere, L., Himber, C., Rinnert, E., Riviere, G., Lambert, C., Soudant, P., Huvet, A., Duflos, G., Paul-Pont, I., 2016.

Microplastics in seafood: benchmark protocol for their extraction and characterization. Environ. Pollut. 215, 223–233.
Eriksen, M., Lebreton, L.C.M., Carson, H.S., Thiel, M., Moore, C.J., Borerro, J.C., Galgani, F., Ryan, P.G., Reisser, J., 2014. Plastic pollution in the world's oceans: more than 5 trillion plastic pieces weighing over 250,000 tons afloat at sea. PLoS One 9 (12), 111913.
European Chemicals Agency (ECHA), 2019. Annex XV Restriction Report Proposal for a Restriction. Report Version Number 1 (March 20th 2019). Helsinki.
Fayolle, B., Richaud, E., Colin, X., Verdu, J., 2008. Degradation-induced embrittlement in semi-crystalline polymers having their amorphous phase in rubbery state. J. Mater. Sci. 43 (22), 6999–7012.
Fazey, F.M., Ryan, P.G., 2016. Biofouling on buoyant marine plastics: an experimental study into the effect of size on surface longevity. Environ. Pollut. 210, 354–360.
Gardette, M., Perthue, A., Gardette, J.L., Janecska, T., Földes, E., Pukánszky, B., Therias, S., 2013. Photo- and thermal-oxidation of polyethylene: comparison of mechanisms and influence of unsaturation content. Polym. Degrad. Stab. 98 (11), 2383–2390.
Graca, B., Szewc, K., Zakrzewska, D., Dołęga, A., Szczerbowska-Boruchowska, M., 2017. Sources and fate of microplastics in marine and beach sediments of the southern Baltic Sea—a preliminary study. Environ. Sci. Pollut. Res. 24, 7650–7661.
Gregory, M.R., Andrady, A.L., 2003. Plastics in the marine environment. In: Andrady, A. L. (Ed.), Plastics and the Environment. John Wiley & Sons Inc, New Jersey, pp. 379–401.
Harris, P.T., 2020. The fate of microplastic in marine sedimentary environments: a review and synthesis. Mar. Pollut. Bull. 158, 111398.
Hermoso, A., Homar, V., Amengual, A., 2021. The sequence of heavy precipitation and flash flooding of 12 and 13 september 2019 in eastern Spain. Part I: mesoscale diagnostic and sensitivity analysis of precipitation. J. Hydrometeorol. 22 (5), 1117–1138.
Hofko, B., Porot, L., Cannone, A.F., Poulikakos, L., Huber, L., Lu, X., Mollenhauer, K., Grothe, H., 2018. FTIR spectral analysis of bituminous binders: reproducibility and impact of ageing temperature. Mater. Struct. 51 (2), 1–16.
Isobe, A., Uchiyama-Matsumoto, K., Uchida, K., Tokai, T., 2017. Microplastics in the Southern Ocean. Mar. Pollut. Bull. 114 (1), 623–626.
Kaci, M., Sadoun, T., Cimmino, S., 2001. Crystallinity measurements of unstabilized and HALS-stabilized LDPE films exposed to natural weathering by FT-IR, DSC and WAXS analyses. Int. J. Polym. Anal. Charact. 6 (5), 455–464.
Kershaw, P., Turra, A., Galgani, F., 2019. Guidelines for the Monitoring and Assessment of Plastic Litter in the Ocean-GESAMP Reports and Studies No. 99. GESAMP Reports and Studies.
Konechnaya, O., Schwanen, C., Schwarzbauer, J., 2021. Application of multi-step approach for comprehensive identification of microplastic particles in diverse sediment samples. Water Sci. Technol. 83 (3), 532–542.
Kühn, S., Van Werven, B., Van Oyen, A., Meijboom, A., Rebolledo, E.L.B., Van Franeker, J.A., 2017. The use of potassium hydroxide (KOH) solution as a suitable approach to isolate plastics ingested by marine organisms. Mar. Pollut. Bull. 115 (1–2), 86–90.
Kurtela, A., Antolović, N., 2019. The problem of plastic waste and microplastics in the seas and oceans: impact on marine organisms. Ribar. Croat. J. Fish. 77 (1), 51–56.
Liu, G., Zhu, Z., Yang, Y., Sun, Y., Yu, F., Ma, J., 2019. Sorption behavior and mechanism of hydrophilic organic chemicals to virgin and aged microplastics in freshwater and seawater. Environ. Pollut. 246, 26–33.
Liu, X., Sun, P., Qu, G., Jing, J., Zhang, T., Shi, H., Zhao, Y., 2021. Insight into the characteristics and sorption behaviors of aged polystyrene microplastics through three type of accelerated oxidation processes. J. Hazard. Mater. 407, 124836.
Lusher, A.L., O'Donnell, C., Officer, R., O'Connor, I., 2016. Microplastic interactions with North Atlantic mesopelagic fish. ICES J. Mar. Sci. 73 (4), 1214–1225.
Maes, T., Van der Meulen, M.D., Devriese, L.I., Leslie, H.A., Huvet, A., Frère, L., Robbens, J., Vethaak, A.D., 2017. Microplastics baseline surveys at the water surface and in sediments of the north-East Atlantic. Front. Mar. Sci. 4, 135.
Matsuguma, Y., Takada, H., Kumata, H., Kanke, H., Sakurai, S., Suzuki, T., Itoh, M., Okazaki, Y., Boonyatumanond, R., Zakaria, M.P., Weerts, S., Newman, B., 2017. Microplastics in sediment cores from Asia and Africa as indicators of temporal trends in plastic pollution. Arch. Environ. Contam. Toxicol. 73 (2), 230–239.
Mellor, D.C., Moir, A.B., Scott, G., 1973. The effect of processing conditions on the UV stability of polyolefins. Eur. Polym. J. 9 (3), 219–225.
Miranda, M.N., Sampaio, M.J., Tavares, P.B., Silva, A.M., Pereira, M.F.R., 2021. Aging assessment of microplastics (LDPE, PET and uPVC) under urban environment stressors. Sci. Total Environ. 796, 148914.
Moore, C.J., 2008. Synthetic polymers in the marine environment: a rapidly increasing, long-term threat. Environ. Res. 108 (2), 131–139.
Niu, L., Li, Y., Li, Y., Hu, Q., Hu, J., Wang, C., Zhang, W., Hu, J., Zhang, W., Wang, L., Zhang, C., Zhang, H., 2021. New insights into the vertical distribution and microbial degradation of microplastics in urban river sediments. Water Res. 188, 116449.
PlasticsEurope, 2020. Plastics - the Facts 2020. An Analysis of European Plastics Production, Demand and Waste Data. PlasticsEurope, Brussels. https://www.plasticseurope.org/ Plastics_the_facts-WEB-2020_versionJun21_final.pdf.
Prata, J.C., Reis, V., Paço, A., Martins, P., Cruz, A., da Costa, J.P., Duarte, A.C., Rocha-Santos, T., 2020. Effects of spatial and seasonal factors on the characteristics and carbonyl index of (micro) plastics in a sandy beach in Aveiro, Portugal. Sci. Total Environ. 709, 135892.
Quinn, B., Murphy, F., Ewins, C., 2017. Validation of density separation for the rapid recovery of microplastics from sediment. Anal. Methods 9 (9), 1491–1498.
Rajakumar, K., Sarasvathy, V., Chelvan, A.T., Chitra, R., Vijayakumar, C.T., 2009. Natural weathering studies of polypropylene. J. Polym. Environ. 17 (3), 191–202.
Razeghi, N., Hamidian, A.H., Wu, C., Zhang, Y., Yang, M., 2021. Microplastic sampling techniques in freshwaters and sediments: a review. Environ. Chem. Lett. 1–28.
Ruiz-Álvarez, V., Belmonte-Serrrato, F., García-Marín, R., 2017. Analysis of precipitations trends in the Region of Murcia (Southeast Spain) over the period 1956-2015. In: 6th International Conference on Meteorology and Climatology of the Mediterranean, February, pp. 20–22.
Rutledge, D.N., Barros, A.S., 2002. Durbin-Watson statistic as a morphological estimator of information content. Anal. Chim. Acta 454, 277–295.
Sánchez, C., 2020. Fungal potential for the degradation of petroleum-based polymers: an overview of macro-and microplastics biodegradation. Biotechnol. Adv. 40, 107501.
Sen, S.K., Raut, S., 2015. Microbial degradation of low density polyethylene (LDPE): a review. J. Environ. Chem. Eng. 3 (1), 462–473.
Singh, B., Sharma, N., 2008. Mechanistic implications of plastic degradation. Polym. Degrad. Stab. 93, 561–584.
Stark, N.M., Matuana, L.M., 2004. Surface chemistry and mechanical property changes of wood-flour/high-density-polyethylene composites after accelerated weathering. J. Appl. Polym. Sci. 94 (6), 2263–2273.
Sundar, S., Chokkalingam, L., Roy, P.D., Usha, T., 2021. Estimation of microplastics in sediments at the southernmost coast of India (Kanyakumari). Environ. Sci. Pollut. Res. 28 (15), 18495–18500.
Ter Halle, A., Ladirat, L., Martignac, M., Mingotaud, A.F., Boyron, O., Perez, E., 2017. To what extent are microplastics from the open ocean weathered? Environ. Pollut. 227, 167–174.
Thostenson, E.T., Ziaee, S., Chou, T.W., 2009. Processing and electrical properties of carbon nanotube/vinyl ester nanocomposites. Compos. Sci. Technol. 69, 801–804.
Tofa, T.S., Kunjali, K.L., Paul, S., Dutta, J., 2019. Visible light photocatalytic degradation of microplastic residues with zinc oxide nanorods. Environ. Chem. Lett. 17 (3), 1341–1346.
Veerasingam, S., Saha, M., Suneel, V., Vethamony, P., Rodrigues, A.C., Bhattacharyya, S., Naik, B.G., 2016. Characteristics, seasonal distribution and surface degradation features of microplastic pellets along the Goa coast, India. Chemosphere 159, 496–505.
Vega-Moreno, D., Abaroa-Pérez, B., Rein-Loring, P.D., Presas-Navarro, C., Fraile-Nuez, E., Machín, F., 2021. Distribution and transport of microplastics in the upper 1150 m of the water column at the Eastern North Atlantic Subtropical Gyre, Canary Islands, Spain. Sci. Total Environ. 788, 147802.
Wagner, M., Scherer, C., Alvarez-Muñoz, D., Brennholt, N., Bourrain, X., Buchinger, S., Fries, E., Grosbois, C., Klasmeier, J., Marti, T., Rodriguez-Mozaz, S., Urbatzka, R., Vethaak, A.D., Winther-Nielsen, M., Reifferscheid, G., 2014. Microplastics in freshwater ecosystems: what we know and what we need to know. Environ. Sci. Eur. 26 (1), 12.
Wang, J., Tan, Z., Peng, J., Qiu, Q., Li, M., 2016. The behaviors of microplastics in the marine environment. Mar. Environ. Res. 113, 7–17.
Wang, J., Wang, M., Ru, S., Liu, X., 2019. High levels of microplastic pollution in the sediments and benthic organisms of the South Yellow Sea, China. Sci. Total Environ. 651, 1661–1669.
Wessel, C.C., Lockridge, G.R., Battiste, D., Cebrian, J., 2016. Abundance and characteristics of microplastics in beach sediments: insights into microplastic accumulation in northern Gulf of Mexico estuaries. Mar. Pollut. Bull. 109, 178–183.
Woodall, L.C., Gwinnett, C., Packer, M., Thompson, R.C., Robinson, L.F., Paterson, G.L., 2015. Using a forensic science approach to minimize environmental contamination and to identify microfibres in marine sediments. Mar. Pollut. Bull. 95 (1), 40–46.
Yu, X., Peng, J., Wang, J., Wang, K., Bao, S., 2016. Occurrence of microplastics in the beach sand of the chinese inner sea: the Bohai Sea. Environ. Pollut. 214, 722–730.
Zerbi, G., Gallino, G., Del Fanti, N., Baini, L., 1989. Structural depth profiling in polyethylene films by multiple internal reflection infra-red spectroscopy. Polymers 30 (12), 2324–2327.
Zheng, Y., Li, J., Cao, W., Jiang, F., Zhao, C., Ding, H., Wang, M., Gao, F., Sun, C., 2020. Vertical distribution of microplastics in bay sediment reflecting effects of sedimentation dynamics and anthropogenic activities. Mar. Pollut. Bull. 152, 110885.